Journal Pre-proof

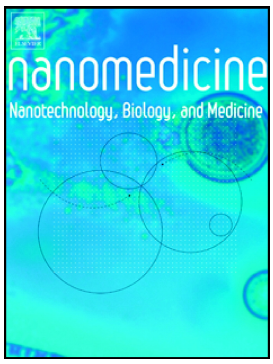

Early-phase Nano-genosensing of cell-free Nucleobiomarkers in the plasma of cancerous patients

Hamidreza Mollasalehi, Asma Hamidi

PII: S1549-9634(20)30198-2

DOI: https://doi.org/10.1016/j.nano.2020.102344

Reference: NANO 102344

To appear in: *Nanomedicine: Nanotechnology, Biology, and Medicine*

Revised date: 16 November 2020

Please cite this article as: H. Mollasalehi and A. Hamidi, Early-phase Nano-genosensing of cell-free Nucleobiomarkers in the plasma of cancerous patients, *Nanomedicine: Nanotechnology, Biology, and Medicine* (2020), https://doi.org/10.1016/j.nano.2020.102344

Early-phase Nano-genosensing of Cell-free Nucleobiomarkers in the Plasma of Cancerous Patients

Hamidreza Mollasalehi, Ph.D.[1]*, and Asma Hamidi, M.Sc.[2]

[1] Department of Cell and Molecular Biology, Faculty of Life Sciences and Biotechnology, Shahid Beheshti University, Tehran, Iran. Postal Code: 1983969411

[2] Protein Research Center, Shahid Beheshti University, Tehran, Iran

Running Title: **Nano-genosensing of cancer nucleobiomarkers**

*Corresponding Author: *Dr. Hamidreza Mollasalehi*

Department of Cell and Molecular Biology, Faculty of life Sciences and Technology, Shahid Beheshti University, Velenjak, Tehran, Iran.

Tel: +98-21-29905942

Fax: +98-21-22431664

E-mail: H_mollasalehi@sbu.ac.ir

Declaration of interests and funding

This work was financially supported by the cancer control research center, cancer control foundation, Iran university of medical sciences, Tehran, Iran, as project No: CCF-97092. The

authors sincerely appreciate the kind providing of the samples by the department of radiotherapy and oncology of Shohada-e-Tajrish Hospital. The authors are also very grateful of the supports by Shahid Beheshti University. The authors declare that they have no known competing financial interests or personal relationships that could have appeared to influence the work reported in this paper.

Abstract wordcount: 150

Complete manuscript wordcount: 4477

Number of references: 36

Number of figures: 4

Number of tables: 0

Abstract:

The extracted miR-21 and miR-155 from the plasma of clinical samples were targeted by non-crosslinking hybridization of Au-nanoprobes without the need for biomarker amplification. Thirty samples, including those suspected to cancer and chemotherapy-treated samples, were analyzed. An increase in the concentration of target biomarkers caused a blue-shift in the visible spectrum of nanoprobes. Using magnesium chloride, the change in the color of nanoprobes was shown to be dependent on time besides intensity. Samples with high averages of intensity needed less time for colorimetric differentiation than those with low average intensity. Au-nanoprobe-21 was turned to purple-gray in clinical specimens of stomach, colon, breast, esophagus, sarcoma, diaphragm, prostate, bladder, lung while Au-nanoprobe-155 appeared as light purple-gray in colon, breast, lung, diaphragm and esophagus samples. The LOD was measured as five ng. μL^{-1} of targeted biomarkers. The developed nano-biosensing method could propose a point-of-care approach for cancer prognosis and diagnosis, facilitating targeted therapeutics.

Keywords: microRNAs; Au-nanoparticles; early-phase diagnosis; extracellular biomarker; nano-biosensor

1. Introduction

A recent analysis of the National Cancer Institute's (NCI) surveillance epidemiology shows that new cases of cancer and new cancer deaths are anticipated in the United States [1, 2]. Cancer is the third most common cause of death in Iran, and 50,000 new cases of cancer occur each year in the Iranian population [3]. Most of the cancers show clinical symptoms in metastasis and final stages. Consequently, choosing effective treatment is hard to achieve. The successful treatment of cancers is dependent on the detection of the disease at its early stages. Detection of biomarkers in bio-fluids such as plasma, saliva, urine is considered as a non-invasive way of cancer early diagnosis [4]. In that regard, the selection of an appropriate cancer biomarker should be made in a way that could pave the way for early detection of cancer.

Circulating cell-free nucleic acids such as miRNA, ncRNA, DNA are considered as suitable biomarkers for non-invasive diagnosis of cancer screening [5] because they are quickly and cheaply detectable in serum or urine. Changes in the levels of circulating tumor markers have been associated with tumor progression. Among the biomarkers, miRNA is a type of small ncRNA that well serves as a circulating tumor marker because of critical roles in differentiation, proliferation, metastasis and apoptosis that mostly appear in the early stages of cancer. miRNA can be protected from degradation by its packaging into exosomes, such as micro-vesicles. Extracellular vehicles (EVs) are found in different biofluids and carry different macromolecules, including proteins, lipid, and nucleic acid [6-11]. Their stability and resistance to degradation in spite of the increased amounts of circulating RNases in the blood of cancerous patients, make them suitable candidates for cancer diagnosis. Abnormal expression of particular miRNAs was found to be involved in differentiating types of cancers such as breast, colon, lung, stomach, prostate cancers. MiRNAs may be downregulated in cancer cells while they act as tumor

suppressing agents in normal tissues. Furthermore, it may be upregulated in some cells in which they have oncogene activity [6, 12, 13]. In that regard, the screening tool must be capable of sensing minimal amount of changes in miRNA concentrations. Early-stage cancer detection could be achieved using miR-155 and miR-21 as detecting probes and nanoparticles as sensors [14-21].

Gold nanoparticle-based colorimetric assay is a sensitive, specific, reproducible, and simple method for the diagnosis of cancer biomarkers in low concentration of liquid biopsies. The exceptional physical properties of Au-NPs such as localized surface plasmon resonance (LSPR) make them useful and potential of bio-sensing platform application in colorimetric assays [16, 20, 22-26]. In this study, we developed an Au-NP-based colorimetric genosensor with non-crosslinking nanoprobes for the detection of selected nucleobiomarkers in the plasma of cancerous clinical samples. We made a quantitative analysis of color-changing of each nanoprobe with regard to time of aggregation and intensity of blue shift.

2. Methods

2.1. Reagents and sampling

Gold-nano particles were synthesized by a joint laboratory of Saman Chemical Technology (Iran). The oligonucleotide synthesis was performed by Bioneer (South Korea). Silica columns were purchased from Proteogenix (France). All chemicals were at the molecular biology grade and purchased from Merck (Germany) except Guanidium thiocyanate, Octanoic Acid, and H_2O_2, which were purchased from Sigma (USA). Blood samples, used in this study, were obtained from the department of radiotherapy and oncology of Shohada-e-Tajrish hospital (Iran). Blind sampling (with no name) was used for all participating patients and approved by Shahid Beheshti

University committee for ethics in biological sciences. The study was performed in accordance with the Declaration of Helsinki.

2.2. Probe design, preparation of Au-NProbes, and characterizations tests

The terminals of 5p in the sequences of miR-21 and miR-155 were targeted for probe design using the *miR-Base* database. Probe1 sequence (targeting miR-21) was 5'TCAACATCAGTCTGATAAGCTA3' and probe2 sequence (targeting miR-155) was 5'ACCCCTATCACGATTAGCATTAA3'. The probes were synthesized with 5' alkane thiol group in the form of a disulfide bond. For reducing residual 5' disulfide bond, oligonucleotide of stock solution (100 µM) was mixed with Tris(2-carboxyethyl) phosphine (0.5 mM), followed by adding nuclease-free water to dilute the final solution. After standing for 1h at RT, colloidal Au-NPs were added to the solution and allowed to stand for 16h. The Au-NProbe solution was salt aged with 18μL of a stock containing NaCl (1M and final concentration of 0.1 M), phosphate buffer (pH: 7, 0.1 M and final concentration of 0.01 M) in four steps. After standing for 48h at RT, the Au-NProbe solution was centrifuged at 11000 g for 35 min followed by removing the supernatant and washing the red pellet with a stock solution containing NaCl (1 M) and phosphate buffer (0.1 M). The mixture was recentrifuged at 11000 g for 35 min, and the supernatant was removed carefully. The washing step was repeated once more to remove unconjugated oligonucleotides. Finally, the pellet was resuspended (redispersed) in 30μL of a buffer containing NaCl (1 M) and phosphate buffer (pH: 7, 100 mM), and stored at 4°C. Characterization tests including FT-IR, zeta potential test, dynamic light scattering (DLS), and UV-Vis spectroscopy were done to check successful conjugation of Au-NPs to oligonucleotide probes. Besides, the miR-21 (5' TAGCTTATCAGACTGATGTTGA 3') and miR-155 (5'

TTAATGCTAATCGTGATAGGGGT 3') sequences which were reverse complementary sequences of each nanoprobe were synthesized and utilized for reliability test.

2.3. miRNA isolation from plasma and storage

A sample of 150μL of plasma was mixed with 230μL of a lysis buffer containing guanidine thiocyanate, TCEP, octanoic acid, and sodium acetate (pH: 4). It was vortexed vigorously, incubated at RT and centrifugated at 10000 g for 3 min. After centrifugation, the supernatant was transferred to a silica column; ethanol was added and centrifuged at 8000 g for 2 min. The column was washed two times by washing buffer. Finally, the TE buffer was added to the column and centrifuged at 4000 g for 15 min. The wash-through solution containing miRNA was transferred to a new tube and stored at -20°C for short-term usage.

2.4. Hybridization assay

Prior to the hybridization assay, the mean concentration of samples was normalized to 10 ng. μL^{-1} for miR-21 and 12 ng. μL^{-1} for miR-155. For detecting miR-155 and miR-21 in total extracted RNA, a hybridization assay was performed by mixing 1.5μL of extracted miRNA with 3μL of Au-NProbes. After mixing, the solution was incubated at 65°C for 4 min and then 40°C for 10 min using a heat block. After hybridization, 0.5μL $MgCl_2$ (0.5M) was added to the solution for differentiating between test positive and negative samples by non-crosslinking gold nanoprobes assay. Once $MgCl_2$ salt was added to the solution, the time and intensity of color-changing were recorded for each sample.

2.5. Statistics and data analysis

Continuous clinical variables, including time and intensity, were analyzed by independent-samples T-Test followed by the Shapiro-wilk test in which P-values < 0.05 was considered meaningful and showed non-uniform distribution of data. To check the normal distribution of data, non-parametric tests, including the Kolmogorov-Smirnov test, were utilized. Consequently, the obtained data were normalized and P-values < 0.05 were achieved. All experiments were carried out using at least three identical repeats.

3. Results

Plasma samples from thirty cancerous patients at their first stages of chemotherapy and suspected cancerous patients were tested using gold nano-biosensor assay by analyzing the effect of time and intensity of color-changing in Au-NProbe-21 and Au-NProbe-155.

3.1. Characterization of Au-NPs/NProbes

To investigate the SPR peaks of Au-NPs, UV-vis spectra were collected using scanning mode ranged between 300-800 nm. The spectra of Au-NP demonstrated an absorbance peak of 524 nm indicating colloidal state and lack of aggregation (Figure 1A). DLS analysis was performed to determine the size distribution of Au-NPs. It was shown that the average diameter of the Au-NPs was 23.30 nm in monodisperse state (PDI: 0.5) (Figure 1B). To investigate the changes between Au-NP and Au-Nprobe colloidal solution, FT-IR and zeta potential tests were performed for both Au-NP (without functionalization) and Au-NProbe conjugates. FT-IR diagram and absorption spectra of Au-NProbe in comparison with Au-NP revealed two peaks at 1233 cm^{-1} and 1110 cm^{-1} [27, 28]. The first peak was related to ribose moiety of oligonucleotides conjugated to Au-NPs, and the second peak was correlated to the phosphate group of conjugated oligonucleotides (Figure 1C I, II). The Au-NPs stabled by citrate exhibited zeta potential of -29.1 mV while the

functionalized Au-NPs with oligonucleotide had a zeta potential of -21 mV (pH: 6-7) (Figure 1D I, II). The charge density alteration at the surface of Au-NP upon functionalization could serve as the basis for a change in zeta potential [29].

3.2. Colorimetric assay

Functionalized Au-NPs were used for nano-biosensing of miR-21 and miR-155 in plasma of cancerous patients. Hybridization of Au-NProbes with short-length target oligonucleotides causes a negatively charged polymeric lattice with reduced electrostatic and steric repulsion resulting in Au-NProbes aggregation in high salt concentrations. The aggregation is followed by a color-changing and a change in the wavelength of absorbance [15, 30]. In that regard, under all constant experimental conditions for samples, both the intensity and timing of the color change from red to violet are dependent on the concentration of the target oligonucleotide.

The study of miR-21 in all tested samples revealed a high expression of this biomarker (high intensity of color-changing from red to violet in lower time) compared to negative samples (Figure 2). For example, stomach cancer sample had an intensity of 0.358, and esophagus cancer showed 0.258. On the other hand, the miR-155 biomarker was differently expressed in various cancers. Bladder, prostate, and sarcoma samples were not increased and had concentrations of 0.04, 0.05, and 0.04, respectively, while this biomarker was raised in the plasma of lung, esophagus, breast, and colon cancer to 0.110, 0.109, 0.135, and 0.146, respectively.

To test the reliability of the method, we hybridized each nanoprobe to its reverse complementary target sequence at a mean concentration of 10 ng. μL^{-} and performed the colorimetric assay under identical experimental condition. It was demonstrated that both Au-Nprobe 1 and Au-Nprobe 2 turned to purple almost instantly while the blank sample comprising ddH_2O instead of

target sequence maintained the red color. The results showed that the nanoprobes could successfully match and hybridize their known target sequences (Supplementary Figure. 1).

3.3. Evaluating the time and intensity of the colorimetric assay

The difference between the average time of color-changing of samples tested with Au-NProbe-21 compared to positive samples tested with Au-NProbe-155 (breast, colon, esophagus, lung, and stomach) is negligible. For instance, the color-changing of Au-NProbe-21 and Au-NProbe-155 was developed in 4.1s and 4.3s for breast cancer, 3.8s, and 3.5s for colon cancer, 3.5s, and 3.5s for lung samples, respectively (Figure 3). It should be noted that there was no color-changing of Au-NProbe-155 in the suspected cancer samples of sarcoma, bladder, and prostate at first seconds, while after 10 seconds, the color was changed from red to light purple. This could be correlated to the lower concentration of miR-155 in those cancers in comparison with the negative control.

To investigate the intensity of color-changing, the absorption spectra of the samples were recorded at 600 nm. The average intensity of color-changing in the presence of two miR-21 and miR-155 were investigated. The measured intensity in lung, breast, and colon cancers was 0.102, 0.147, and 0.126, respectively for Au-NProbe-21, and 0.110, 0.135, and 0.140, respectively for Au-NProbe-155. Therefore, significantly the measured intensity for both probes was almost equal. On the other hand, the average intensity of color-changing of bladder, prostate, and sarcoma during testing with Au-NProbe-155 was decreased in comparison with negative control (0.06, 0.05, 0.04) and it was increased compared to the negative control using Au-NProbe-21 (0.145, 0.188, 0.13) (Figure2).

The samples are categorized into two groups, including the plasma of suspected cancerous patients and chemotherapy-treated specimens. The intensity of color-changing was investigated for both miR-21 and mirR-155 regarding the type of samples. The expression levels of both biomarkers were increased in all kinds of cancers in the suspected groups in comparison with chemotherapy samples. This implies that chemotherapy treatment was effective in the investigated patients. For example, the optical density of color-changing for the suspected and chemotherapy colon samples tested by Au-NProbe-21 was 0.145 and 0.120, respectively. It should be noted that bladder and sarcoma specimens of chemotherapy-treated samples were found to show more intensive color-changing (blue-shift) than suspected cases (Figure 4).

4. Discussion

The conventional methods for detecting cancers such as physical examination, ultrasonography, positron emission tomography (PET) scan, computerized axial tomography (CT) scan, colonoscopy, endoscopy, and taking biopsy are almost time-consuming costly methods that have low sensitivity and specificity [31-35]. On the other hand, most of the cancers present the clinical symptoms in the final-phases. Therefore, neither early-phase diagnosis nor effective treatment of cancer happen. That is why nucleobiomarkers in the plasma of cancerous patients seem to be a golden key for the case of early-phase cancer theranostics using nano-genosensors. In this study, non-cross-linking aggregation of gold nanoparticles was utilized for quantitative analysis of time and intensity of color-changing of Au-NProbes in two groups of suspected cancerous and chemotherapy-treated samples. It was shown that the color of Au-NProbe-21 was changed from red to purple-gray in clinical specimens of stomach, colon, breast, esophagus, sarcoma, diaphragm, prostate, bladder, and lung samples, while the color-changing of Au-NProbe-155 appeared as light purple-gray in colon, breast, lung, diaphragm, and esophagus samples.

However, there was no color-changing of Au-NProbe-155 for bladder, prostate, and sarcoma, indicating that the amount of miR-155 was decreased in these cancers. This could be probably due to the role of miR-155 as tumor suppressors in bladder, prostate, and sarcoma cancers. In that regard, in a study on the breast cancer samples, miRNA-155 was detected using graphene oxide and electrochemical gold nanorod biosensor. Direct detection of miR-155 in the plasma was done without RNA extraction, and the measured LOD was 0.6 fM [34]. In another study on the plasma of cancer patients including breast, colorectal, and lung samples, miR-21 was detected by Au-NProbes with a crosslinking aggregation method, and LOD was measured as 0.5 fM [17].

The time needed for color development of Au-NProbe-21 and Au-NProbe-155 was also examined, and it was shown that samples with high averages of intensity required less time for colorimetric differentiation than those with low proportions of intensity. For example, the color alternation of stomach samples with the highest intensity of miR-21 was observable in less than three seconds (the minimum time of color-changing). In addition, the samples with high-concentration of miR-155 showed nearly the same time of color-changing as miR-21 compared to three negative control samples. The samples with higher intensity and lower time of color-changing are prone to more successful early-phase detection. For instance, the intensity of breast cancer samples was more than of colon samples, and the color-changing of breast cancer samples was developed in a lower required time. Therefore, breast cancer is of higher potential of being detected in the early stages. To the best of our knowledge, this is the first report on the investigation of both time and intensity of color-changing in non-crosslinking Au-NProbes aggregation of clinical samples.

Interestingly, it was found that the level of expression of miR-21 biomarker in most cancers (e.g. stomach, colon, breast, lung, esophagus, sarcoma, prostate and bladder) and miR-155 expression

in some investigated cancers including esophagus, colon, breast, lung and stomach were relatively high in not only the suspected cancer patients but also in chemotherapy-treated patients after 4-5 treatment stages. This could be due to a failure in the chemotherapy treatment, and/or unusual miRNA leakage from cells into bloodstream, and/or metastasis.

It was previously shown that miR-21 was increased in the lung, breast, colon, ovarian, thyroid, and gastric cancer cell lines using a non-crosslinking aggregation method, while miR-155 was only increased in the lung, breast, colon, ovarian, and thyroid cancer cell lines with LOD of one ng. μL^{-1}. In this study, real clinical samples were used to measure the concentration of the nucleobiomarkers using the colorimetric nano-biosensing method. It was shown that miR-21 was increased in all tested cancers, including suspected and chemotherapy-treated samples, though miR-155 was only increased in lung, breast, colon, esophagus, stomach samples. The measured LOD was five ng. μL^{-1} because of the lower concentration of miRNAs in clinical samples. It should be noted that LOD of the assay was determined as the least concentration of target miRNA that could induce visual color differentiation by naked eyes.

Accuracy- a ratio of the experimental value to the actual value of a substance in a matrix- seems to be a challenging issue for POC testing. This study was based on two schemes to conquer the issue. First, we aimed to target appropriate biomarker(s) potential of early-detection (to prognose and diagnose cancers). Therefore, circulating exosomal miRNAs dysregulation was utilized as there were evidences that they are expressed precedingly to affect signal transduction systems and expression of specific genes prior to phenotypic changes in the late stages of cancer [35, 36]. Subsequently, an effective approach for sensing the concentration changes of the biomarkers with high sensitivity was nominated. In that regard, nanoparticle-based assay with the sensitivity

as low as aM/fM of the target was applied. The developed methodology could serve as a screening approach prior to biopsy prescription even for non-symptomatic patients at risk.

In conclusion, the non-crosslinking LSPR diagnostic method as a nano-biosensor (facilitated by salt addition) could assist fast and straightforward diagnosis of diseases. The designed nano-biosensor is potential of both qualitative diagnosis of cancers at early stages and also the quantitative study of different stages with the analysis of time and intensity of color alterations. This methodology not only could help simple, rapid diagnosis of cancers but also could pave the way for accurate theranostic approaches. In that regard, the validity of the method was investigated by examining different clinical samples in their various stages of progression and healing. This method could well serve as a kind of point-of-care and cost-effective approach for early detection of cancer cells.

Conflict of interest

The authors declare that there is no competing financial interest regarding the manuscript content and no conflict of interest.

Ethics approval

This study was approved by Shahid Beheshti University committee for ethics in biological sciences with the committee's reference number: IR.SBU.REC.1398. The study was performed in accordance with the Declaration of Helsinki. Blind sampling (with no name) was used for all participating patients.

Data availability

The authors confirm that the data supporting the findings of this study are available within the article and/or its supplementary materials.

Authorship

HM designed the experiment, interpreted the results and helped write the manuscript. AH did the experiment, analyzed the data and wrote the first draft of the manuscript.

6. References:

R. L. Siegel, K. D. Miller and A. Jemal, **Cancer statistics, 2017**. *CA: a cancer journal for clinicians*. 2017;67:7-30

R. A. Smith, A. C. von Eschenbach, R. Wender, B. Levin, T. Byers, D. Rothenberger, et al., **American Cancer Society guidelines for the early detection of cancer: update of early detection guidelines for prostate, colorectal, and endometrial cancers: Also: update 2001—testing for early lung cancer detection**. *CA: a cancer journal for clinicians*. 2001;51:38-75

M. Mohebbi, M. Mahmoodi, R. Wolfe, K. Nourijelyani, K. Mohammad, H. Zeraati, et al., **Geographical spread of gastrointestinal tract cancer incidence in the Caspian Sea region of Iran: spatial analysis of cancer registry data**. *BMC cancer*. 2008;8:137

M. S. Pepe, R. Etzioni, Z. Feng, J. D. Potter, M. L. Thompson, M. Thornquist, et al., **Phases of biomarker development for early detection of cancer**. *Journal of the National Cancer Institute*. 2001;93:1054-1061

L. O'DRISCOLL, **Extracellular nucleic acids and their potential as diagnostic, prognostic and predictive biomarkers**. *Anticancer research*. 2007;27:1257-1265

T. Paranjape, F. Slack and J. Weidhaas, **MicroRNAs: tools for cancer diagnostics**. *Gut*. 2009;58:1546-1554

S. Fichtlscherer, S. De Rosa, H. Fox, T. Schwietz, A. Fischer, C. Liebetrau, et al., **Circulating microRNAs in patients with coronary artery diseasenovelty and significance**. *Circulation research*. 2010;107:677-684

G. Shafiee, R. Heshmat and B. Larijani, **Circulating cell-free nucleic acids as potential biomarkers for sarcopenia: a step toward personalized medicine**. *Journal of Diabetes & Metabolic Disorders*. 2017;16:19

F. Momen-Heravi, S. J. Getting and S. A. Moschos, **Extracellular vesicles and their nucleic acids for biomarker discovery**. *Pharmacology & therapeutics*. 2018

H. Valadi, K. Ekström, A. Bossios, M. Sjöstrand, J. J. Lee and J. O. Lötvall, **Exosome-mediated transfer of mRNAs and microRNAs is a novel mechanism of genetic exchange between cells**. *Nature cell biology*. 2007;9:654

E. A. Lekchnov, I. A. Zaporozhchenko, E. S. Morozkin, O. E. Bryzgunova, V. V. Vlassov and P. P. Laktionov, **Protocol for miRNA isolation from biofluids**. *Analytical biochemistry*. 2016;499:78-84

J. Ahmad, S. E. Hasnain, M. A. Siddiqui, M. Ahamed, J. Musarrat and A. A. Al-Khedhairy, **MicroRNA in carcinogenesis & cancer diagnostics: a new paradigm**. *The Indian journal of medical research*. 2013;137:680

Y. Peng and C. M. Croce, **The role of MicroRNAs in human cancer**. *Signal transduction and targeted therapy*. 2016;1:15004

G. Wang, Y. Akiyama, S. Shiraishi, N. Kanayama, T. Takarada and M. Maeda, **Cross-linking versus non-cross-linking aggregation of gold nanoparticles induced by DNA hybridization: A comparison of the rapidity of solution color change**. *Bioconjugate chemistry*. 2016;28:270-277

W. Zhao, M. A. Brook and Y. Li, **Design of gold nanoparticle-based colorimetric biosensing assays**. *ChemBioChem*. 2008;9:2363-2371

S. Lim, O. K. Koo, Y. S. You, Y. E. Lee, M.-S. Kim, P.-S. Chang, et al., **Enhancing nanoparticle-based visible detection by controlling the extent of aggregation**. *Scientific reports*. 2012;2:456

L. Guo, Y. Lin, C. Chen, B. Qiu, Z. Lin and G. Chen, **Direct visualization of sub-femtomolar circulating microRNAs in serum based on the duplex-specific nuclease-amplified oriented assembly of gold nanoparticle dimers**. *Chemical Communications*. 2016;52:11347-11350

K. Sato, K. Hosokawa and M. Maeda, **Rapid aggregation of gold nanoparticles induced by non-cross-linking DNA hybridization**. *Journal of the American Chemical Society*. 2003;125:8102-8103

W. Xu, X. Xue, T. Li, H. Zeng and X. Liu, **Innentitelbild: Ultrasensitive and Selective Colorimetric DNA Detection by Nicking Endonuclease Assisted Nanoparticle Amplification (Angew. Chem. 37/2009)**. *Angewandte Chemie*. 2009;121:6870-6870

X. Miao, X. Ning, Z. Li and Z. Cheng, **Sensitive detection of miRNA by using hybridization chain reaction coupled with positively charged gold nanoparticles**. *Scientific reports*. 2016;6:32358

H. Mollasalehi and R. Yazdanparast, **An improved non-crosslinking gold nanoprobe-NASBA based on 16S rRNA for rapid discriminative bio-sensing of major salmonellosis pathogens**. *Biosensors and Bioelectronics*. 2013;47:231-236

L. M. Zanoli, R. D'Agata and G. Spoto, **Functionalized gold nanoparticles for ultrasensitive DNA detection**. *Analytical and bioanalytical chemistry*. 2012;402:1759-1771

J. J. Storhoff, R. Elghanian, R. C. Mucic, C. A. Mirkin and R. L. Letsinger, **One-pot colorimetric differentiation of polynucleotides with single base imperfections using gold nanoparticle probes**. *Journal of the American Chemical Society*. 1998;120:1959-1964

J. J. Storhoff, R. Elghanian, C. A. Mirkin and R. L. Letsinger, **Sequence-dependent stability of DNA-modified gold nanoparticles**. *Langmuir*. 2002;18:6666-6670

J. J. Storhoff, A. A. Lazarides, R. C. Mucic, C. A. Mirkin, R. L. Letsinger and G. C. Schatz, **What controls the optical properties of DNA-linked gold nanoparticle assemblies?** *Journal of the American Chemical Society*. 2000;122:4640-4650

K. Zeng, H. Li and Y. Peng, **Gold nanoparticle enhanced surface plasmon resonance imaging of microRNA-155 using a functional nucleic acid-based amplification machine**. *Microchimica Acta*. 2017;184:2637-2644

A. B. D. Nandiyanto, R. Oktiani and R. Ragadhita, **How to read and interpret FTIR spectroscope of organic material**. *Indonesian Journal of Science and Technology*. 2019;4:97-118

L. Spevak, C. R. Flach, T. Hunter, R. Mendelsohn and A. Boskey, **Fourier transform infrared spectroscopic imaging parameters describing acid phosphate substitution in biologic hydroxyapatite**. *Calcified tissue international*. 2013;92:418-428

A. J. Shnoudeh, I. Hamad, R. W. Abdo, L. Qadumii, A. Y. Jaber, H. S. Surchi, et al., 2019. Synthesis, Characterization, and Applications of Metal Nanoparticles *Biomaterials and Bionanotechnology*, Elsevier, pp. 527-612

T. Mori and M. Maeda, **Stability change of DNA-carrying colloidal particle induced by hybridization with target DNA**. *Polymer journal*. 2002;34:624-628

A. Gallamini, C. Zwarthoed and A. Borra, **Positron emission tomography (PET) in oncology**. *Cancers*. 2014;6:1821-1889

H. K. Ha, P. J. Koo and S.-J. Kim, **Diagnostic accuracy of F-18 FDG PET/CT for preoperative lymph node staging in newly diagnosed bladder cancer patients: a systematic review and meta-analysis**. *Oncology*. 2018;95:31-38

J. M. Huguet, P. Suárez, L. Ferrer-Barceló, L. Ruiz, A. Monzó, A. B. Durá, et al., **Endoscopic recommendations for colorectal cancer screening and surveillance in patients with inflammatory bowel disease: Review of general recommendations**. *World journal of gastrointestinal endoscopy*. 2017;9:255

M. Azimzadeh, M. Rahaie, N. Nasirizadeh, K. Ashtari and H. Naderi-Manesh, **An electrochemical nanobiosensor for plasma miRNA-155, based on graphene oxide and gold nanorod, for early detection of breast cancer**. *Biosensors and Bioelectronics*. 2016;77:99-106

E. Shajari and H. Mollasalehi, **Ribonucleic-acid-biomarker candidates for early-phase group detection of common cancers**. *Genomics*. 2020;112:163-168

H. Wang, R. Peng, J. Wang, Z. Qin and L. Xue, **Circulating microRNAs as potential cancer biomarkers: the advantage and disadvantage**. *Clinical epigenetics*. 2018;10:1-10

Figure legends:

Figure 1. Characterization tests of Au-NPs and Au-NProbes. **A**: UV-Visible spectra of Au-NPs and the absorbance peak at 520 nm. **B**: DLS analysis of Au-NPs showing the monodisperse distribution of the Au-NPs. **C I**: FT-IR diagram of the Au-NPs. No absorption peak was observed. **C II**: FT-IR diagram of Au-NProbes. Two adsorption peaks were observed at 1233 cm-1 and 1110 cm-1. **D I**: Zeta potential of Au-NPs. The stabled gold nanoparticles showed a zeta potential of -29.1 mv. **D II**: Zeta potential of Au-NProbes showing a zeta potential of -21 mV.

Figure 2. The average intensity of color alteration in clinical samples at 600 nm. All samples tested by Au-NProbe-21 resulted in higher intensities than negative samples. All samples tested by Au-NProbe-21 resulted in higher intensities than negative samples. However, different intensities were recorded by Au-NProbe-155. A value of $p < 0.05$ was considered statistically significant.

Figure 3. The time of color alteration of Au-NProbe-21 and Au-NProbe-155 tested on cancer samples. Samples with low miR-155 such as sarcoma needed much more time for color-changing. A value of $p < 0.05$ was considered statistically significant.

Figure 4. The intensity of color-changing in chemotherapy-treated cancer samples in comparison with suspected cancer samples tested by Au-NProbe-21 and Au-NProbe-155. A value of $p < 0.05$ was considered statistically significant.

CRediT author statement

Hamidreza Mollasalehi: Conceptualization, Methodology, Supervision, Writing- Reviewing and Editing, Project administration, Funding acquisition. **Asma Hamidi**: Investigation, Writing- Original draft preparation.

Graphical Abstract

Schematic representation of the Au-nanoprobe assay method. The colorimetric detection is based on the non-crosslinking hybridization of Au-nanoprobes in the presence of complementary miRNA-21 and miRNA-155 and occurs in a timely manner. Induction of aggregation using magnesium chloride improves the differentiation stage of the assay by decreasing the required time for color-changing from red to purple.

A

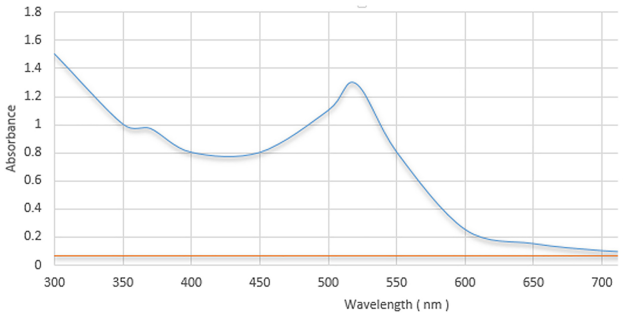

B

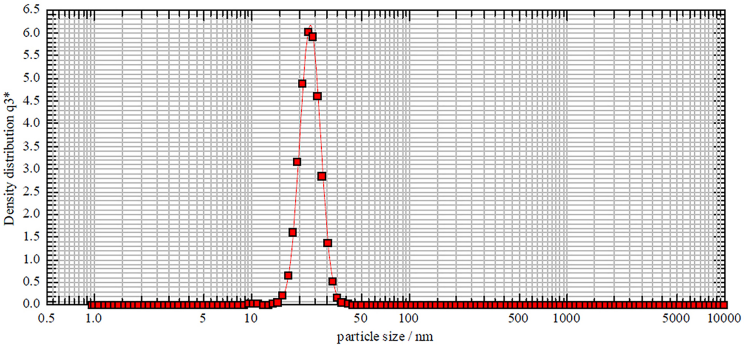

C I

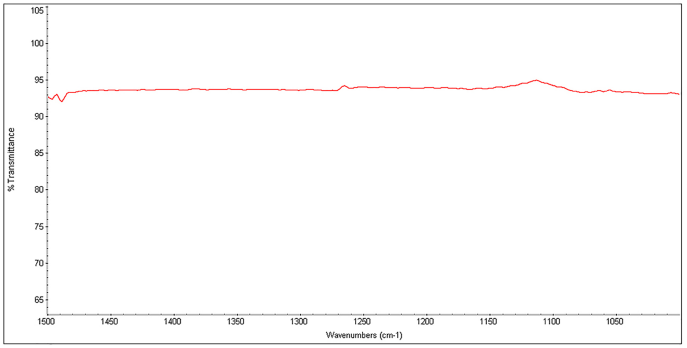

C II

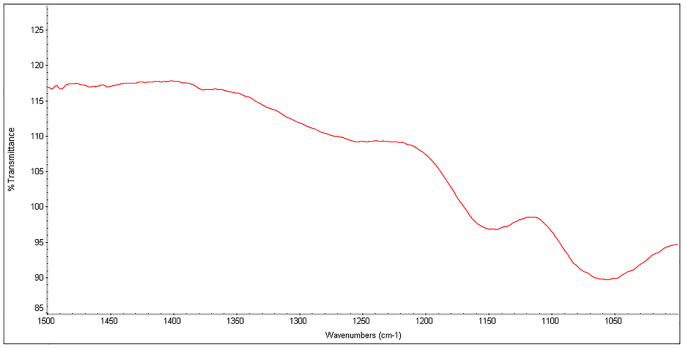

D I

		Mean (mV)	Area (%)	Width (mV)
Zeta Potential (mV): -29.1	Peak 1:	-29.1	100.0	5.16
Zeta Deviation (mV): 5.16	Peak 2:	0.00	0.0	0.00
Conductivity (mS/cm): 0.136	Peak 3:	0.00	0.0	0.00

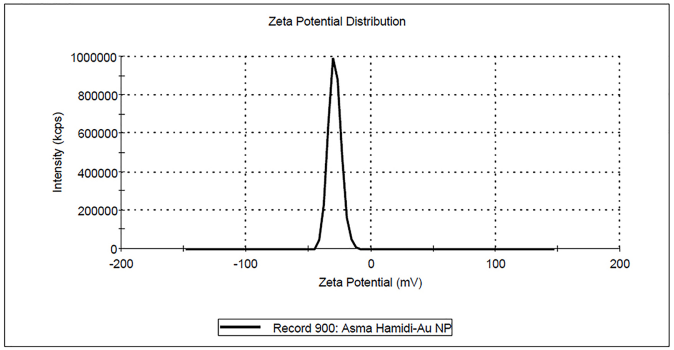

D II

		Mean (mV)	Area (%)	Width (mV)
Zeta Potential (mV): -21.0	Peak 1:	-21.0	100.0	5.04
Zeta Deviation (mV): 5.04	Peak 2:	0.00	0.0	0.00
Conductivity (mS/cm): 0.0460	Peak 3:	0.00	0.0	0.00

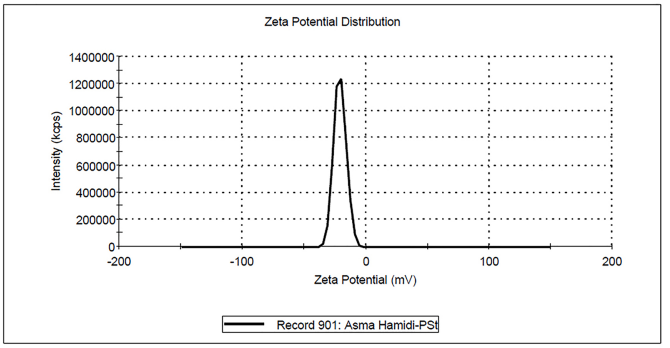

Figure 1

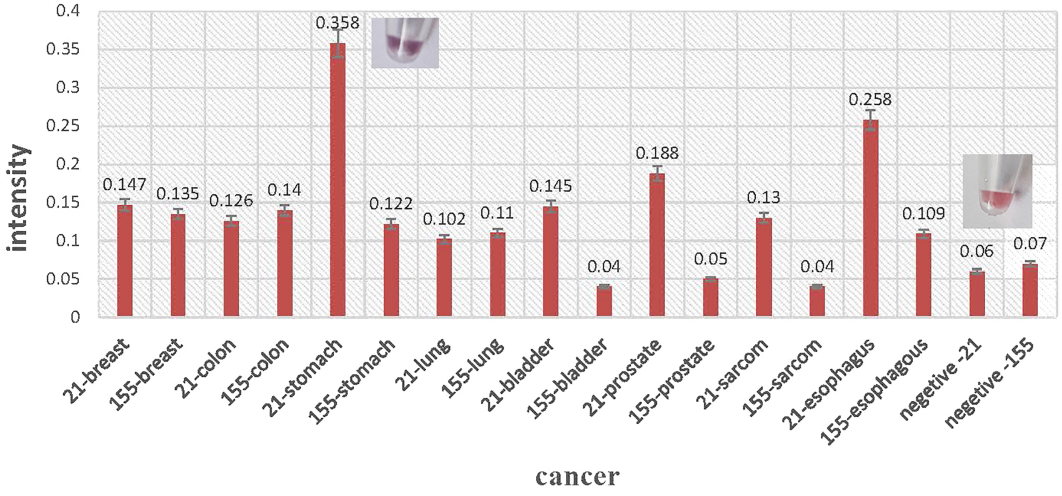
intensity
0.4
0.35
0.3
0.25
0.2
0.15
0.1
0.05
0
0.147
0.135
0.126
0.14
0.358
0.122
0.102
0.11
0.145
0.04
0.188
0.05
0.13
0.04
0.258
0.109
0.06
0.07
21-breast
155-breast
21-colon
155-colon
21-stomach
155-stomach
21-lung
155-lung
21-bladder
155-bladder
21-prostate
155-prostate
21-sarcom
155-sarcom
21-esophagus
155-esophagous
negetive -21
negetive -155
cancer

Figure 2

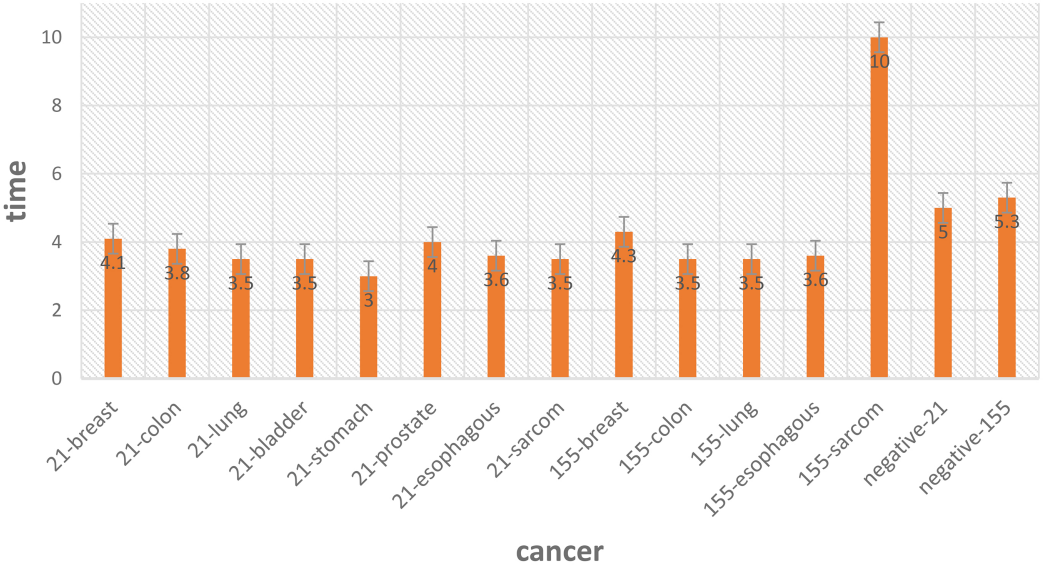
time
10
8
6
4
2
0
4.1
3.8
3.5
3.5
3
4
3.6
3.5
4.3
3.5
3.5
3.6
10
5
5.3
21-breast
21-colon
21-lung
21-bladder
21-stomach
21-prostate
21-esophagous
21-sarcom
155-breast
155-colon
155-lung
155-esophagous
155-sarcom
negative-21
negative-155
cancer

Figure 3

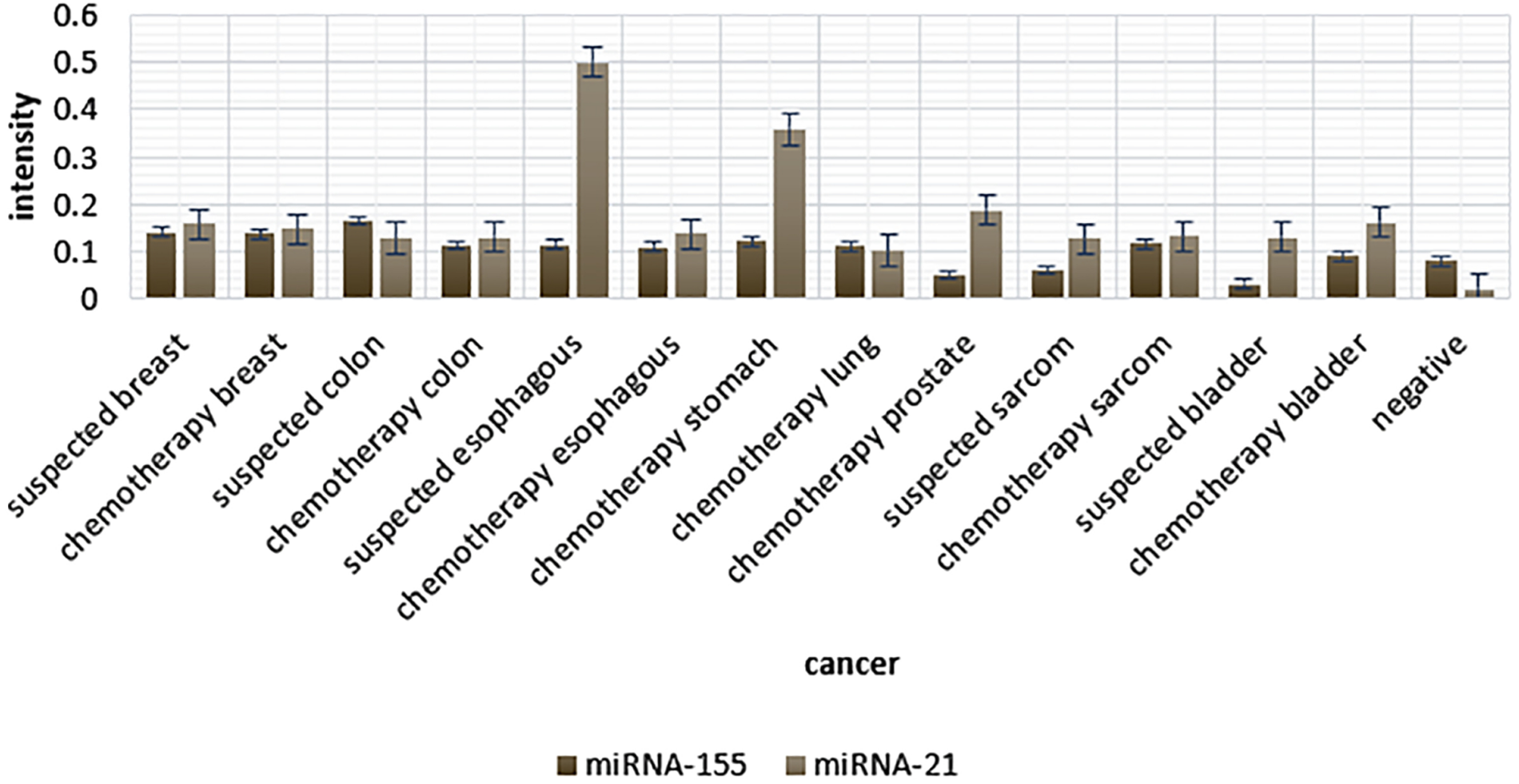
0.6
0.5
0.4
0.3
0.2
0.1
0
intensity
suspected breast
chemotherapy breast
suspected colon
chemotherapy colon
suspected esophagous
chemotherapy esophagous
chemotherapy stomach
chemotherapy lung
chemotherapy prostate
suspected sarcom
chemotherapy sarcom
suspected bladder
chemotherapy bladder
negative
cancer
miRNA-155
miRNA-21

Figure 4